Scaling hypothesis leading to generalized extended self-similarity in turbulence

Hirokazu Fujisaka* and Yasuya Nakayama†
Department of Applied Analysis and Complex Dynamical Systems, Graduate School of Informatics, Kyoto University, Kyoto 606-8501, Japan

Takeshi Watanabe‡
Division of Global Development Science, Graduate School of Science and Technology, Kobe University, Kobe 657-8501, Japan

Siegfried Grossmann§
Fachbereich Physik, Philipps Universität, Renthof 6, D-35032 Marburg, Germany

(Received 27 June 2001; revised manuscript received 3 December 2001; published 10 April 2002)

A scaling hypothesis leading to generalized extended self-similarity (GESS) for velocity structure functions, valid for intermediate scales in isotropic, homogeneous turbulence, is proposed. By introducing an effective scale $\hat{r}$, monotonically depending on the physical scale r, with the use of the large deviation theory, the asymptotic forms of the probability densities for the velocity differences u_r and for the coarse-grained energy-dissipation rate fluctuations ϵ_r, compatible with this GESS, are proposed. The probability density for ϵ_r is shown to have the form $P_r(\epsilon)\sim\epsilon^{-1}(\hat{r}/L)^{S_{\hat{r}}^{\hat{}}(z_{\hat{r}}^{\hat{}}(\epsilon))}$ with $z_{\hat{r}}^{\hat{}}(\epsilon)=\ln(\epsilon/\epsilon_L)/\ln(L/\hat{r})$, where L and ϵ_L are the stirring scale and the coarse-grained energy-dissipation rate over the scale L. The concave function $S_{\hat{r}}^{\hat{}}(z)$, the spectrum, plays the central role of the present approach. Comparing the results with numerical and experimental data, we explicitly obtain the fluctuation spectra $S_{\hat{r}}^{\hat{}}(z)$.

DOI: 10.1103/PhysRevE.65.046307 PACS number(s): 47.27.Gs, 47.27.Eq, 47.27.Jv

I. INTRODUCTION

One of the main topics of studies on developed turbulence is about velocity structure functions in isotropic, homogeneous turbulence that are believed to show universal statistics in small scales in between the Kolmogorov microscale (viscous scale) η and the stirring (energy injection) scale L [1]. The velocity structure function is defined as

$$S_q^u(r)\equiv\langle u_r^q(\mathbf{x})\rangle, \tag{1.1}$$

where

$$u_r(\mathbf{x})\equiv|\mathbf{v}_l(\mathbf{r}+\mathbf{x})-\mathbf{v}_l(\mathbf{x})|, \quad r\equiv|\mathbf{r}|, \tag{1.2}$$

is the difference of the longitudinal velocity components at two points separated by the distance r, and the angular brackets denote the ensemble average. Statistical homogeneity and isotropy of turbulence imply that its statistics depends on neither the position $\mathbf{x}$ nor the direction vector $\mathbf{r}/r$, provided that the positions $\mathbf{x}$ and $\mathbf{x}+\mathbf{r}$ are far from the boundary of the fluid container. It is believed that the structure function $S_q^u(r)$ obeys the power law [1,2]

$$S_q^u(r)\sim r^{\zeta(q)}, \tag{1.3}$$

in the so-called inertial subrange $\eta<r<L$, provided it is sufficiently wide. The width of the inertial subrange is determined by the Reynolds number $\mathrm{Re}=u_L L/\nu$ with the characteristic velocity u_L of the fluid at the outer scale L and the kinematic viscosity ν,

$$\frac{L}{\eta}\sim\mathrm{Re}^{3/4}. \tag{1.4}$$

The similarity hypothesis of Kolmogorov [3], using dimensional arguments, gives

$$\zeta_{K41}(q)=\frac{q}{3}. \tag{1.5}$$

The derivation of this formula is based on the assumption that the energy-dissipation rate is a scale independent constant in the inertial subrange (ISR). Its validity was questioned because of the strong fluctuations of the energy-dissipation rate in space and time. This is called the intermittency problem and is one of the most interesting problems in turbulence [1].

Introducing the coarse-grained energy-dissipation rate $\epsilon_r(\mathbf{x})$ by

$$\epsilon_r(\mathbf{x})\equiv\frac{1}{(4\pi r^3/3)}\int_{|\mathbf{y}|<r}\epsilon_{local}(\mathbf{y}+\mathbf{x})d\mathbf{y}, \tag{1.6}$$

with the local energy-dissipation rate per mass

$$\epsilon_{local}(\mathbf{x})=\frac{\nu}{2}\sum_{i,j}\left(\frac{\partial v_i(\mathbf{x})}{\partial x_j}+\frac{\partial v_j(\mathbf{x})}{\partial x_i}\right)^2, \tag{1.7}$$

in 1962, Kolmogorov [4] and Obukhov [5] assumed that $\epsilon_r(\mathbf{x})$ is statistically related to $u_r(\mathbf{x})$ via

*Email address: fujisaka@i.kyoto-u.ac.jp
†Email address: nakayama@acs.i.kyoto-u.ac.jp
‡Present address: Department of Systems Engineering, Nagoya Institute of Technology, Nagoya 466-8555, Japan. Email address: watanabe@system.nitech.ac.jp
§Email address: grossmann@physik.uni-marburg.de

$$\frac{u_r}{u_L} \sim \left(\frac{\epsilon_r}{\epsilon_L}\right)^{1/3} \left(\frac{r}{L}\right)^{1/3} \tag{1.8}$$

up to a statistically irrelevant numerical factor. Here $\epsilon_L \equiv u_L^3/L$ is the energy-dissipation rate averaged over the largest available scale, the outer scale L, assumed to show no fluctuations. If we define the coarse-grained energy-dissipation rate structure function $S_q^\epsilon(r)$ and assume the asymptotic law [2]

$$S_q^\epsilon(r) \equiv \langle \epsilon_r^q(\mathbf{x}) \rangle \sim r^{\tau(q)}, \tag{1.9}$$

in the inertial subrange, the combination of Eqs. (1.3), (1.8), and (1.9) yields

$$\zeta(q) = \frac{q}{3} + \tau\left(\frac{q}{3}\right). \tag{1.10}$$

The dissipation rate scaling exponent function $\tau(q)$ thus describes the deviation from the Kolmogorov scaling $\zeta_{K41}(q) = q/3$, see Eq. (1.5), and it is determined by the fluctuation statistics of $\epsilon_r(\mathbf{x})$. We have

$$\tau(0) = 0, \quad \tau(1) = 0, \quad \text{and} \quad \tau(2) \equiv -\mu. \tag{1.11}$$

The first equation is trivial, the second reflects the structure equation, which gives $\zeta(3) = 1$ (and is related to the statistical homogeneity of the turbulent field). The third equation is the definition of the intermittency exponent μ (with $\mu > 0$), which is one of the parameters characterizing the fluctuations of $\epsilon_r(\mathbf{x})$.

One of the fundamental problems of the statistical theory of turbulence is to determine the velocity scaling exponent functions $\zeta(q)$ and $\tau(q)$. Although many studies have been carried out about $\zeta(q)$ both experimentally and theoretically, we still have no conclusive experimental results and no solid theoretical basis about $\zeta(q)$ [2]. The experimental difficulties are the limited statistics and/or the limited Reynolds numbers. The theoretical problem is the nonlinearity of the Navier-Stokes equation.

In 1993 Benzi *et al.* [6] noticed a surprising and interesting fact about the velocity structure functions $S_q^u(r)$. These authors pointed out that even if the Reynolds number is not sufficiently large and, therefore, the power law (1.3) is not distinctly developed, still power law relations hold over a wide r range, namely, between different order velocity structure functions $S_q^u(r)$ and $S_p^u(r)$ for arbitrary pairs q and p. This discovery, called the extended self-similarity (ESS), enables us to measure the function $\zeta(q)$ more precisely than with Eq. (1.3) [7,8]. Furthermore, in 1996 Benzi *et al.* [9,10] discovered an even more generalized form of ESS, which seems to hold in an even wider r range than ESS. They called it the generalized extended self-similarity (GESS). After these discoveries, numerous experimental or numerical analyses of structure functions based on ESS and GESS have been published [11]. Although ESS and GESS are experimentally quite effective to analyze data, their theoretical basis remained unsatisfactorily clarified. In Ref. [12], we proposed a phenomenological derivation of the ESS formulas. The aim of the present paper is to extend that. We formulate ESS and GESS by applying the large deviation theory, and we also calculate the relevant statistical quantities by analyzing numerical and experimental data.

The paper is organized as follows. In Sec. II, we briefly review ESS and GESS, and discuss the general forms of the velocity structure functions and of the energy-dissipation rate structure functions that explain ESS and GESS. In Sec. III, postulating a generalization of the refined similarity hypothesis, we propose a similarity theory of the energy-dissipation rate fluctuations by applying the large deviation theory. We show that the asymptotic statistics of the velocity difference fluctuations and of the energy-dissipation rate fluctuations, as determined by the functions $\tilde{f}(r)$ and $\tilde{g}_1(r)$, turn out to agree with the experimentally found ESS and GESS. In Sec. IV, utilizing data from numerical simulations of Navier-Stokes flows and from experiments in jet flows, these functions are explicitly determined. Furthermore, the experimentally obtained fluctuation spectrum $S_{\hat{r}}(z)$ is compared with that based on existing phenomenological theories. Finally, discussion and remarks are given in Sec. V.

II. ESS AND GESS

In 1993, Benzi *et al.* empirically found that even if because of small or moderate Reynolds numbers the inertial subrange with its power law behavior is not sufficiently extended, the following relation holds in an r range, which is larger than in a plot of $S_q^u(r)$ vs r,

$$S_q^u(r) \sim [S_p^u(r)]^{\alpha(q|p)}. \tag{2.1}$$

The exponent $\alpha(q|p)$ is a unique function depending only on q and p. This relation was reported for various moment orders q,p and for numerical simulations as well as for experimental measurements. Since, in the inertial subrange, relation (2.1) has to be compatible with Eq. (1.3), one obtains

$$\alpha(q|p) = \frac{\zeta(q)}{\zeta(p)}. \tag{2.2}$$

Therefore, if one exponent $\zeta(p)$ is known, e.g., $\zeta(3) = 1$, the precise observation of $\alpha(q|p)$ yields $\zeta(q)$. This fact is known as ESS.

The relation (2.1) implies that $S_q^u(r)$ generally takes the form [10,12]

$$S_q^u(r) \sim u_L^q \left[\frac{r}{L}\tilde{g}_1(r)\right]^{\zeta(q)}, \tag{2.3}$$

where $\tilde{g}_1(r)$ is a dimensionless function of r, which is independent of the moment order q. Inversely, Eq. (2.3) leads to Eq. (2.1). Although originally ESS was thought to hold in a range extending the ISR toward smaller scales, i.e., into the viscous subrange (VSR), detailed numerical analyses showed that instead it extended toward larger r scales, i.e., beyond the crossover region between the inertial and the stirring subranges [13]. In addition, it has been reported that the broader extension toward large scales can also be observed in two-

dimensional magnetohydrodynamic turbulence [14]. Therefore, it seems quite natural to assume that the dimensionless function $\tilde{g}_1(r)$ depends on r in terms of the outer scale L (instead of η, the inner, viscous, Kolmogorov scale),

$$\tilde{g}_1(r)=g\left(\frac{r}{L}\right). \tag{2.4}$$

The scaling function $g(x)$ is expected to be universal, i.e., to be the same for different moment orders q and different experiments. This assumption gives

$$S_q^u(r)\sim u_L^q\left[\frac{r}{L}g\left(\frac{r}{L}\right)\right]^{\zeta(q)}. \tag{2.5}$$

This will be checked numerically and experimentally in Sec. IV, with a $g(x)$ satisfying $g(x)=1$ for $x\ll 1$ and $g(x)=x^{-1}$ for $x\gg 1$.

In the previous paper [12] we extended the refined similarity hypothesis (1.8) by introducing a scaling exponent $\overline{z_r}$ [15] by

$$\epsilon_r\sim\epsilon_L\left[\frac{r}{L}g\left(\frac{r}{L}\right)\right]^{-\overline{z_r}}, \tag{2.6}$$

$$u_r\sim u_L\left[\frac{r}{L}g\left(\frac{r}{L}\right)\right]^{(1/3)(1-\overline{z_r})}. \tag{2.7}$$

From the postulates (2.6) and (2.7) one immediately derives

$$\frac{u_r}{u_L}\sim\left(\frac{\epsilon_r}{\epsilon_L}\right)^{(1/3)}\left[\frac{r}{L}g\left(\frac{r}{L}\right)\right]^{(1/3)}. \tag{2.8}$$

This extends, cf. Refs. [10,12], the similarity hypothesis (1.8) of Kolmogorov and Obukhov. We there fore call it the extended refined similarity hypothesis (ERSH). One should note that Eq. (2.8) is to be understood in a statistical sense. If r can be chosen sufficiently smaller than L but still sufficiently larger than η, Eq. (2.8) reduces to Eq. (1.6), because here $g(x)=1$. However, the r dependence becomes visible, if either there exists no broad ISR because of an only moderate Reynolds number or if r is chosen near the outer scale L. Evaluating S_q^u from Eq. (1.1) by combining Eqs. (2.8), (2.3), and (1.10), one finds

$$S_q^\epsilon(r)\sim\epsilon_L^q\left[\frac{r}{L}g\left(\frac{r}{L}\right)\right]^{\tau(q)}. \tag{2.9}$$

Therefore, we can conclude that ERSH leads to ESS for the energy-dissipation rate structure function too,

$$S_q^\epsilon(r)\sim[S_p^\epsilon(r)]^{\beta(q|p)}, \tag{2.10}$$

where in this case

$$\beta(q|p)=\frac{\tau(q)}{\tau(p)}. \tag{2.11}$$

The characteristics of ESS may be summarized as follows.

(i) $\zeta(q)$ can be determined already from turbulent flow with only moderate Re.

(ii) The structure functions of the velocity differences and of the coarse-grained dissipation rates obey the scaling laws (2.5) and (2.9) with a single function $g(x)$, which may be universal.

(iii) ESS is valid in the crossover region from the inertial (ISR) to the stirring (SSR) subranges.

Some years ago, Benzi *et al.* [10] furthermore found experimentally that the compensated velocity structure functions $G_{q,3}(r)$ satisfy $G_{q,3}(r)\sim[G_{q',3}(r)]^{\rho_{q,q'}}$ with $\rho_{q,q'}=[\zeta(q)-q/3]/[\zeta(q')-q'/3]$, where

$$G_{q,p}(r)\equiv\frac{S_q^u(r)}{(S_p^u(r))^{q/p}}. \tag{2.12}$$

This suggests that a generalization, denoted as GESS,

$$G_{q,p}(r)\sim[G_{q',p'}(r)]^{\gamma(q,p|q',p')}, \tag{2.13}$$

might hold for a wider range even if a power law, cf. Eq. (1.3), is not yet developed. Here $\gamma(q,p|q',p')$ is considered as independent of r and as a unique function of the moment orders q, p, q', and p'. Since Eq. (2.13) holds in particular in the inertial subrange, where $S_q^u(r)$ has the power law dependence (1.3) on r, one expects the relation

$$\gamma(q,p|q',p')=\frac{\frac{q}{p}\zeta(p)-\zeta(q)}{\frac{q'}{p'}\zeta(p')-\zeta(q')}=\frac{\frac{q}{p}\tau\left(\frac{p}{3}\right)-\tau\left(\frac{q}{3}\right)}{\frac{q'}{p'}\tau\left(\frac{p'}{3}\right)-\tau\left(\frac{q'}{3}\right)}. \tag{2.14}$$

Here we used the relation (1.10). Thus with GESS one may directly measure the relative ratio of the excess exponent $\tau(q)$. For further details on the compensated plots of $S_q^u(r)$ see Refs. [13,16,17].

The observation (2.13) implies that the velocity structure functions $S_q^u(r)$ take the even more general form than Eq. (2.3), namely,

$$S_q^u(r)\sim u_L^q[\tilde{f}(r)]^q\left[\frac{r}{L}\tilde{g}_1(r)\right]^{\zeta(q)}, \tag{2.15}$$

where $\tilde{f}(r)$ and $\tilde{g}_1(r)$ are dimensionless functions of r, and are independent of the moment order q. In fact, it is easily shown that Eq. (2.13) holds for any choice of the functions $\tilde{f}(r)$ and $\tilde{g}_1(r)$, if only these do not depend on q. The functions $\tilde{f}(r)$ and $r\tilde{g}_1(r)$ in Eq. (2.15) correspond respectively to $[F(r)/G(r)]^{1/3}$ and $G(r)$ in Eq. (52) of Ref. [10].

The structure functions $S_q^u(r)$ must have the asymptotic forms

$$S_q^u(r)\sim\begin{cases} r^q & (r\ll l),\\ \text{ESS scaling (2.5)} & (r\gg l).\end{cases} \tag{2.16}$$

Here l denotes the inner crossover scale of the turbulent flow, above which the inertial subrange starts. l is a multiple of the Kolmogorov length η,

$$l \equiv a\,\eta, \tag{2.17}$$

the parameter a being about 10 [18]. The first asymptotics in Eq. (2.16) must hold because the velocity difference u_r in the viscous subrange is proportional to the scale r itself. In order to meet Eq. (2.16), the dimensionless functions $\tilde{f}(r)$ and $\tilde{g}_1(r)$ must satisfy

$$\tilde{f}(r) = \begin{cases} c_1 \dfrac{r}{l} & (r \ll l), \\ c_2 & (r \gg l), \end{cases}$$
$$\tilde{g}_1(r) = \begin{cases} c_3 \left(\dfrac{r}{l}\right)^{-1} & (r \ll l), \\ g\left(\dfrac{r}{L}\right) & (r \gg l), \end{cases} \tag{2.18}$$

where c_1, c_2, c_3 are positive constants of order unity, and $g(x)$ is the same as in Eq. (2.4). For the VSR-ISR crossover statistics, see Ref. [19]. The characteristic features of GESS may be summarized as follows.

(i) $\zeta(q)$ can be determined even in moderate Re number turbulence.

(ii) The scaling laws (2.13) and (2.15) are characterized by two functions $\tilde{f}(r)$ and $\tilde{g}_1(r)$, which may be universal.

(iii) GESS is the bridging formula for all three subranges, the viscous, the inertial, and the stirring subranges.

In the following section, we will derive GESS from a phenomenological ansatz in a generalized way as was previously done for ESS, see Ref. [12].

III. GENERALIZED EXTENDED REFINED SIMILARITY HYPOTHESIS AND GENERALIZED EXTENDED SELF-SIMILARITY

The Navier-Stokes equations are invariant under the transformation [20,2,12]

$$r' = br, \quad u_{r'} = b^{(1/3)(1-\bar{z})} u_r, \quad t' = b^{(1/3)(2+\bar{z})} t,$$
$$p_{r'} = b^{(2/3)(1-\bar{z})} p_r, \quad \epsilon_{r'} = b^{-\bar{z}} \epsilon_r, \quad \nu' = b^{(1/3)(4-\bar{z})} \nu, \tag{3.1}$$

where p_r is the characteristic pressure difference over the linear scale r, ν is the kinematic viscosity, b is an arbitrary positive constant, and $\bar{z}$ an arbitrary exponent. This invariance might suggest to introduce the scaling hypotheses

$$\epsilon_r \sim \epsilon_L \left[\frac{r}{L}\tilde{g}_1(r)\right]^{-\bar{z}_r}, \tag{3.2}$$

$$u_r \sim u_L \tilde{f}(r) \left[\frac{r}{L}\tilde{g}_1(r)\right]^{(1/3)(1-\bar{z}_r)}. \tag{3.3}$$

Here $\tilde{f}(r)$ and $\tilde{g}_1(r)$ are arbitrary, dimensionless functions of r. As will be shown later, they coincide with the functions $\tilde{f}$ and $\tilde{g}_1$ in the preceding section. $\bar{z}_r$ is assumed to be a random variable, whose statistics, which expresses the $\epsilon_r(\mathbf{x})$ and the $u_r(\mathbf{x})$ statistics, will be defined later. Equations (3.2) and (3.3) give

$$\frac{u_r}{u_L} \sim \left(\frac{\epsilon_r}{\epsilon_L}\right)^{1/3} \tilde{f}(r) \left[\frac{r}{L}\tilde{g}_1(r)\right]^{1/3}. \tag{3.4}$$

Equations (3.2), (3.3), and (3.4), generalizing Eqs. (2.6), (2.7), and (2.8), will be called the generalized extended refined similarity hypotheses (GERSH). They are expected to be valid for all scales, including those above L as well as those below l. The scaling hypotheses (3.2) and (3.3) together with the large deviation theory of probability theory [21–23] will play the central role in deriving the GESS formula (2.15).

First we introduce an effective scale $\hat{r}$ by

$$\hat{r}(r) \equiv r\tilde{g}_1(r), \tag{3.5}$$

where $\hat{r}(r)$ is assumed to be a monotonously increasing function of r, $\hat{r}'(r) > 0$. This implies that Eq. (3.5) is a one-to-one transformation between r and $\hat{r}$. The transformation generally is nonlinear.

Then, let us define discrete scales by

$$\frac{\hat{r}_n}{L} \equiv \frac{r_n}{L}\tilde{g}_1(r_n) = b^{-n}, \quad n = 0,1,2,\ldots,N, \tag{3.6}$$

where b with $b > 1$ is an arbitrarily chosen number.

$$N = -\log_b \left[\frac{l}{L}\tilde{g}_1(l)\right] \tag{3.7}$$

is associated with the finiteness of the microscale η, and is assumed to be sufficiently large.

Introduce now exponents z_n by

$$\frac{\epsilon_{r_{n+1}}}{\epsilon_{r_n}} = b^{-z_n}, \quad n = 0,1,\ldots,N. \tag{3.8}$$

The properties of the set $\{z_n\}$ will characterize the self-similarity of the energy-dissipation rate fluctuations. It is understood that the z_n obey the same statistics for all n and do not have any statistical anomalies, as, e.g., divergent variances or the like, for $0 \leq n \leq N$. This is considered as the explicit mathematical expression of self-similarity that holds in the range of scales $l < r < L$. Equation (3.8) can be solved to yield

$$\epsilon_{r_n} = \epsilon_L b^{-n\bar{z}_n}. \tag{3.9}$$

Here ϵ_L describes the $n = 0$ dissipation rate, and $\bar{z}_n$ is the coarse-grained exponent defined by

$$\overline{z}_n=\frac{1}{n}\sum_{j=0}^{n-1} z_j . \tag{3.10}$$

The combination of Eqs. (3.9) and (3.6) gives $\epsilon_{r_n}\sim\epsilon_L[(r_n/L)\tilde{g}_1(r_n)]^{-\overline{z}_n}$, and therefore the exponents $\overline{z}_n$ coincide with $\overline{z}_{r_n}$ in Eqs. (3.2) and (3.3). The important point is that the variables $\overline{z}_n$ are defined in terms of a set of random variables $\{z_j\}$ with j independent statistics. Incidentally, this condition can be generalized in such a way that the correlation along the series of successive z_j is finite and much smaller than the step n under consideration. This fact enables us to apply the large deviation theoretical analysis in evaluating the statistics of ϵ_{r_n}. We can, for large n, introduce the characteristic function $\tau(q)$ via

$$S_q^{\epsilon}(r_n)=\langle \epsilon_{r_n}^q(\mathbf{x})\rangle=\langle \epsilon_L^q b^{-nq\overline{z}_n(\mathbf{x})}\rangle\equiv\epsilon_L^q b^{-n\tau(q)}. \tag{3.11}$$

Use has been made of the approximation that ϵ_L has no fluctuations. Eliminating b^{-n} via Eq. (3.6) leads to

$$S_q^{\epsilon}(r)=\epsilon_L^q\left[\frac{r}{L}\tilde{g}_1(r)\right]^{\tau(q)}. \tag{3.12}$$

This in turn together with the assumption (3.4) implies Eq. (2.15) including the exponent relation (1.10), and also

$$S_q^u(r)\sim[\tilde{f}(r)]^q\left[\frac{r}{L}\tilde{g}_1(r)\right]^{q/3}S_{q/3}^{\epsilon}(r). \tag{3.13}$$

Eliminating $\tilde{g}_1(r)$ in terms of $S_p^{\epsilon}(r)$, we obtain Eq. (2.10), the exponent being given by Eq. (2.11). Therefore, we can conclude that Eq. (2.10) holds not only in the range where ESS is valid but also in the broader range where GESS holds.

One should note that, since $\overline{z}_n$ is given as the sum of statistically equal random variables, the large deviation theory [21–23] of probability theory implies that the probability densities $Q_n(z)\equiv\langle\delta(\overline{z}_n-z)\rangle$ for $\overline{z}_n$ asymptotically in n obey

$$Q_n(z)\sim\sqrt{n}b^{-S_n(z)n}=\sqrt{n}\left(\frac{\hat{r}_n}{L}\right)^{S_n(z)}, \tag{3.14}$$

where $S_n(z)$ is a concave function of z, i.e., $S_n''(z)>0$, if only n is much larger than the correlation width of the z_n. The exponent $S_{\hat{r}_n}(z)[\equiv S_n(z)]$ is called the Cramer function, also the rate function, or the fluctuation spectrum, and it plays the central role of the large deviation theoretical approach. The prefactor $\sqrt{n}$ is because $S_{\hat{r}_n}(z)$ has a parabolic form near its unique minimum. Although the large deviation theory asserts that $S_n(z)$ is independent of n for $n\to\infty$ provided this limit can be taken, we here retain its n dependence for later discussion.

Abbreviating $\epsilon_n=\epsilon_L b^{-nz}=\epsilon_L(\hat{r}_n/L)^z\equiv\epsilon$, i.e., $\overline{z}_n=\ln(\epsilon_n/\epsilon_L)/\ln(L/\hat{r}_n)\equiv z$, the probability density $P_{r_n}(\epsilon)$ $(=Q_n(z)|dz/d\epsilon|)$ for ϵ_{r_n} is asymptotically given by

$$P_{r_n}(\epsilon)\sim\frac{\epsilon^{-1}}{\sqrt{\ln\frac{L}{\hat{r}_n}}}\left(\frac{\hat{r}_n}{L}\right)^{S_{\hat{r}_n}(z)}. \tag{3.15}$$

One arrives at

$$P_r(\epsilon)\sim\frac{\epsilon^{-1}}{\sqrt{\ln\frac{L}{\hat{r}}}}\left(\frac{\hat{r}}{L}\right)^{S_{\hat{r}}(z_{\hat{r}}(\epsilon))}, \tag{3.16}$$

with

$$z_{\hat{r}}(\epsilon)\equiv\frac{\ln\frac{\epsilon}{\epsilon_L}}{\ln\frac{L}{\hat{r}}}. \tag{3.17}$$

The probability density $P_r(u)[=|d\epsilon/du|P_r(\epsilon)]$ for u_r is straightforwardly given from Eq. (3.16) and the assumption (3.4) as

$$P_r(u)\sim\frac{u^{-1}}{\sqrt{\ln\frac{L}{\hat{r}}}}\left(\frac{\hat{r}}{L}\right)^{S_{\hat{r}}(1+3z_{\hat{r}}(u))}, \tag{3.18}$$

where

$$u=u_L\left(\frac{\epsilon}{\epsilon_L}\right)^{1/3}\tilde{f}(r)\left(\frac{\hat{r}}{L}\right)^{1/3}, \tag{3.19}$$

$$z_{\hat{r}}(u)\equiv\frac{\ln\frac{u}{u_L\tilde{f}(r)}}{\ln\frac{L}{\hat{r}}}\equiv-\frac{1}{3}[1-z_{\hat{r}}(\epsilon)]. \tag{3.20}$$

Appendix A offers a derivation of the asymptotic form (3.16) from a point of view slightly different from the one above, which is based on the self-similarity of the energy-dissipation rate fluctuations.

As also discussed in Appendix A, the fluctuation spectrum $S(z)$ may piecewise take two types of z dependences. The first one is a concave function and the second one is a linear function of z. However, as shown in Sec. IV, numerical and experimental analyses show no feasibility of the second type of solution. So, we hereafter assume that the fluctuation spectrum $S(z)$ is a concave function of z.

The exponent function $\tau(q)$ and the fluctuation spectrum $S(z)$ are related [22,23,12] by

$$\tau(q)=S(z(q))-qz(q), \tag{3.21}$$

where

$$z(q)=-\tau'(q),\quad S'(z(q))=q. \tag{3.22}$$

These quantities, in principle, have r dependences, which, however, we omitted in Eqs. (3.21) and (3.22). If the dissipation rate exponent function $\tau(q)$ is known, the above Legendre transformation enables us to obtain the fluctuation spectrum. On the other hand, one can directly measure $S(z)$, utilizing the asymptotic formulas (3.16) or (3.18) for the dissipation or the velocity difference fluctuations.

The functions $\tilde{f}(r)$,$\tilde{g}_1(r)$, or $S_{\hat{r}}(z)$ may thus describe the asymptotic statistical characteristics of isotropic, homogeneous turbulent flow despite moderate Reynolds numbers. If the Reynolds number is sufficiently large such that the scale r can be chosen well within the ISR, $l \ll r \ll L$, the above formulas reduce to those in developed turbulence. In the following section, we shall determine these functions by analyzing data from numerical simulations and from experiment.

So far the asymptotic form of the probability density $P_r(u)$ for velocity difference fluctuations was discussed by assuming the GERSH. With this assumption it is determined by the fluctuation spectrum $S_{\hat{r}}(z_{\hat{r}}(\epsilon))$ for the energy-dissipation rate fluctuation. The validity of GERSH is, however, not obvious. Without the use of the GERSH, one can derive the asymptotic probability density $P_r(u)$, assuming the self-similarity of velocity difference fluctuations. This is done by applying the procedure similar to the above for energy-dissipation rate fluctuations.

Let us define the exponent $z_n^{(u)}$ via [22]

$$\frac{u_{r_{n+1}}}{u_{r_n}} = b^{-z_n^{(u)}}, \quad n = 0,1,2,\ldots,N, \tag{3.23}$$

where r_n and b are the same as defined in Eq. (3.6), and $z_n^{(u)}$ is assumed to be statistically steady in n and to have a sufficiently short correlation step. This is solved to yield $u_{r_n} = u_L b^{-n\overline{z_n^{(u)}}}$ with $\overline{z_n^{(u)}} = n^{-1}\Sigma_{j=0}^{n-1} z_j^{(u)}$. Applying the large deviation theory, one can define the characteristic function $\tilde{\zeta}(q)$ via $\langle b^{-nq\overline{z_n^{(u)}}}\rangle = b^{-n\tilde{\zeta}(q)}$ and the fluctuation spectrum $S_{\hat{r}}^u(z^{(u)})$, with which the probability density is found to take the asymptotic form

$$P_r(u) \sim \frac{u^{-1}}{\sqrt{\ln \frac{L}{\hat{r}}}} \left(\frac{\hat{r}}{L}\right)^{S_{\hat{r}}^u(z_{\hat{r}}^{(u)}(u))}, \quad z_{\hat{r}}^{(u)}(u) = \frac{\ln \frac{u}{u_L}}{\ln \frac{L}{\hat{r}}}. \tag{3.24}$$

The function $\tilde{\zeta}(q)$ is assumed to depend only on q. If the GERSH is applicable, the relations

$$z_{\hat{r}}^{(u)}(u) = z_{\hat{r}}(u) + \frac{\ln \tilde{f}(r)}{\ln \frac{L}{\hat{r}}}, \tag{3.25a}$$

$$S_{\hat{r}}^u(z_{\hat{r}}^{(u)}(u)) = S_{\hat{r}}(1 + 3z_{\hat{r}}(u)) \tag{3.25b}$$

should hold, where $z_{\hat{r}}(u)$ is the same as that in Eq. (3.20). Particularly, one gets $z_{\hat{r}}^{(u)}(u) = z_{\hat{r}}(u)$ in the ISR. The relation (3.25b) will be tested with experimental data in the following section.

IV. NUMERICAL AND EXPERIMENTAL DETERMINATION OF THE FUNCTIONS CHARACTERIZING ESS AND GESS

In the present section, we compare the results of the phenomenological theory obtained in the preceding sections with those of numerical flow simulations by Fukayama *et al.* and with those of laboratory experiments done by Katsuyama *et al.*

Data A. Direct numerical simulations (Fukayama *et al.* [24]). Fukayama *et al.* [24] carried out direct numerical simulation (DNS) of the three-dimensional Navier-Stokes equations. The data we will use are RUN 5 for forced turbulence in their paper. The numerical procedure is as follows. The number of mesh points is 512^3. As initial condition a Gaussian random velocity field with an energy spectrum $E(k,0) = c(k/k_0)^4 \exp[-2(k/k_0)^2]$ with $k_0 = 3$ is used. The energy is permanently injected with a statistically homogeneous, isotropic, and Gaussian white random force limited to the band $2 \leqslant k \leqslant 3$. The parameter values of the simulations are estimated as

$$\nu \approx 0.001\,35, \quad \epsilon_L \approx 0.492, \quad \eta \approx 0.008\,43, \quad L \approx 1.56,$$
$$\mathrm{Re}_\lambda \approx 125, \quad a \approx 10.8. \tag{4.1}$$

ϵ_L was obtained from its definition (1.6), i.e., by using the spatial derivatives of the velocity field. ϵ_L together with ν then implies η. The number a is defined by $a = l/\eta$, see Eq. (2.17); we estimated the crossover scale between the viscous and inertial subranges to be $l = 0.0910$ by fitting Fukayama *et al.*'s data to the Batchelor parametrization [27,18],

$$S_2^u(r) = \frac{\epsilon_L}{15\nu} r^2 \left[1 + \left(\frac{r}{l}\right)^2\right]^{-1+\zeta(2)/2}. \tag{4.2}$$

The estimate of $\zeta(2)$, done by using the ESS analysis, led to $\zeta(2)/\zeta(3) = 0.692$. Since, in these DNS data, there does not exist a sufficiently extended power law regime, one cannot measure $\zeta(3)$ sufficiently precise. We thus assume $\zeta(3) = 1$ and get $\zeta(2) = 0.692$.

Data B. Jet flow experiment (Katsuyama *et al.* [25,26]) Katsuyama *et al.*'s data [25,26] were measured in an air-in-air jet flow 6.5 m downstream from a square nozzle of size 0.4 m×0.4 m. The axial velocity of the flow was measured at discrete times $t_j = j\Delta t$, $j = 1,2,3,\ldots$, where $\Delta t = 10$ μs is the time interval between neighboring sampling times. The velocity just behind the nozzle was 30 m s^{-1}. The probe's diameter is 5 μm and its hot wire length 700 μm. The output signal was high-pass filtered at the frequency 0.1 kHz. The smallest eddies time scale ($\equiv 10\sqrt{\nu/\epsilon_L}$) is 4 ms, 400 times larger than the resolution. The number of data points is 6×10^5. The mean velocity $U(=u_L)$ at the measuring position was 14.4 m s^{-1}, and the root mean square of the velocity

fluctuations was $v_{\rm rms}=2.9$ m s^{-1}; this value was calculated according to the definition $v_{\rm rms}=\sqrt{\langle (v_j-U)^2\rangle}$, where v_j is the measured velocity at time t_j. Other parameters were evaluated as follows. First we defined the local energy-dissipation rate ϵ_j by

$$\epsilon_j = 15\nu\left(\frac{v_{j+k}-v_j}{kU\Delta t}\right)^2, \tag{4.3}$$

where we put $k=6$, corresponding to about 11 times η, one of the viscous range scales to evaluate the v derivative; average values for smaller ones turned out to approximately give the same values as that for $k=6$. Experimental analysis shows that the time difference $6\Delta t$ is not too short to evaluate the local energy-dissipation rate. So we did not use the low pass filter of velocity fluctuations. The mean dissipation rate ϵ_L was obtained with the formula $\epsilon_L = 15\nu\langle(\partial v_x/\partial x)^2\rangle$; we approximated $\langle(\partial v_x/\partial x)^2\rangle$ by $\langle(v_{j+k}-v_j)^2\rangle/(\Delta x)^2$ with $\Delta x = kU\Delta t$, $k=6$. The Kolmogorov microscale η, the Taylor length λ, and the stirring scale L were calculated using $\eta=(\nu^3/\epsilon_L)^{1/4}$, $\lambda=\sqrt{15\nu v_{\rm rms}^2/\epsilon_L}$, and $L=v_{\rm rms}^3/\epsilon_L$. Finally, the Taylor-Reynolds number is $\mathrm{Re}_\lambda = v_{\rm rms}\lambda/\nu$. The parameter values thus obtained are

$$\nu = 15 \ \text{mm}^2\ \text{s}^{-1},\ \ \epsilon_L \approx 84 \ \text{m}^2\ \text{s}^{-3}, \eta \approx 80\ \mu\text{m},$$

$$L \approx 0.28\ \text{m},\quad \mathrm{Re}_\lambda \approx 900,\ \ a \approx 15. \tag{4.4}$$

The parameter a again was calculated via fit of the data to the Batchelor parametrization (4.2) with $\zeta(2)=0.70\times\zeta(3)=0.70\times 0.97=0.68$ to determine the crossover scale l; this turned out to be $l=1.2$ mm. Furthermore, the coarse-grained energy-dissipation rate ϵ_r was determined as $\epsilon_r = m^{-1}\Sigma_{j=1}^m \epsilon_j$ with $r=mU\Delta t$. The probability density $P_r(\epsilon)$ will be calculated with the ensemble for ϵ_r defined in this way. The spatial resolution $(=U\Delta t)$ is 140 μm, which turns out to be almost twice the Kolmogorov scale.

Figure 1 shows the exponent functions $\zeta(q)/\zeta(3)$ and $\tau(q)=\zeta(3q)/\zeta(3)-q$ for both data A and B. Here the maximum value $q_{max}=4$ for q in Fig. 1 is chosen after estimating the statistical scatter in the relevant tail region of the probability density for the velocity differences u_r, using a standard method, see, e.g., Ref. [24]. The function $\zeta(q)$ for each data set was determined using the ESS plot (2.1) with $p=3$. While for the data A one cannot determine $\zeta(3)$ too precisely, and we therefore assumed $\zeta(3)=1$, for the data B one can measure $\zeta(3)\approx 0.97$. Hereafter, the values of the exponents in Fig. 1 will be used for later analysis of the structure functions. The scaling relation (2.15) can be rearranged to give

$$[S_p^u(r)]^{\zeta(q)/\zeta(p)} \sim u_L^{p[\zeta(q)/\zeta(p)]}[\tilde{f}(r)]^{p[\zeta(q)/\zeta(p)]}\left[\frac{r}{L}\tilde{g}_1(r)\right]^{\zeta(q)}. \tag{4.5}$$

Eliminating $\tilde{g}_1(r)$ from Eqs. (2.15) and (4.5) leads to

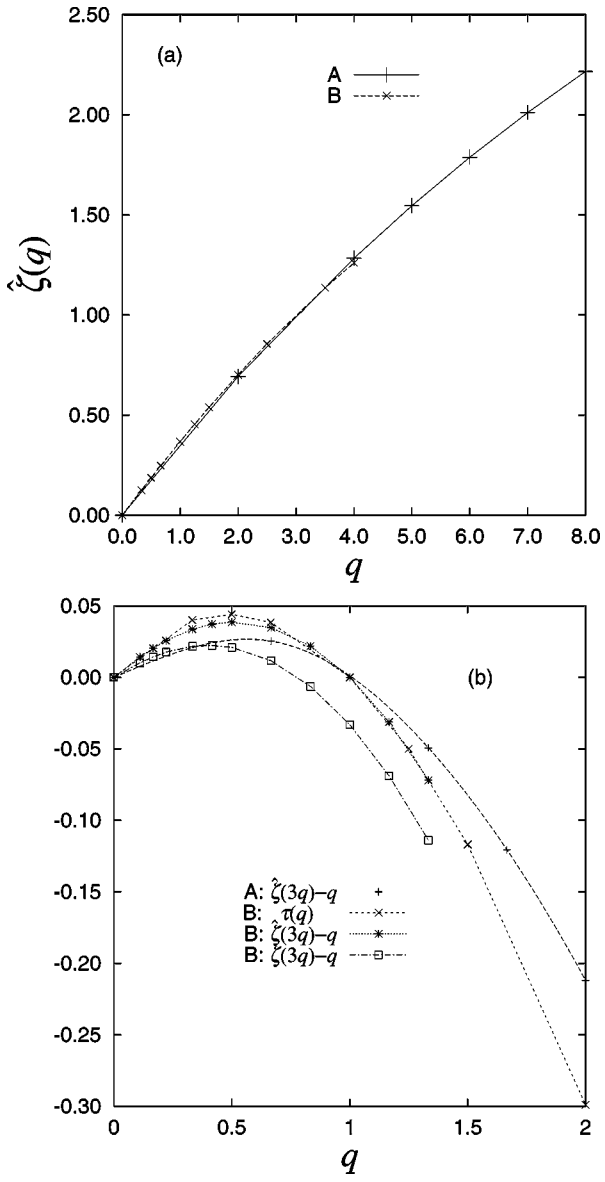

FIG. 1. (a) The exponent function $\hat{\zeta}(q)\equiv\zeta(q)/\zeta(3)$ for data A and B. (b) The functions $\zeta(3q)-q$, $\hat{\zeta}(3q)-q$, and $\tau(q)$ for data A and B. Lines except for $\tau(q)$ are drawn with spline functions.

$$\tilde{f}(r) \sim \{S_q^u(r)[S_p^u(r)]^{-\zeta(q)/\zeta(p)}\}^{1/[q-p\zeta(q)/\zeta(p)]} = \{[S_q^u(r)]^{\zeta(p)}[S_p^u(r)]^{-\zeta(q)}\}^{1/[q\tau(p/3)-p\tau(q/3)]}, \tag{4.6}$$

except for numerical factors. The last expression was obtained with the relation (1.10). If the function $\tilde{f}(r)$ is indeed universal, as we expect and have assumed, the rhs of Eq. (4.6) has to be independent of q and p. In a similar way, inserting Eq. (4.6) into Eq. (2.15), we get

$$\frac{r}{L}\tilde{g}_1(r) \sim \{[S_q^u(r)]^{1/q}[S_p^u(r)]^{-1/p}\}^{1/[\zeta(q)/q-\zeta(p)/p]} = \{[S_q^u(r)]^p[S_p^u(r)]^{-q}\}^{-1/[q\tau(p/3)-p\tau(q/3)]}. \tag{4.7}$$

The last expression was also obtained with the relation (1.10). Again, if $\tilde{g}_1(r)$ exists as a universal scaling function, the rhs of Eq. (4.7) must be independent of q and p, too. From these equations (4.6) and (4.7) we then can numerically determine $\tilde{f}(r)$ and $\tilde{g}_1(r)$ as functions of either r/L or of

$$r^* \equiv \frac{r}{\eta}. \tag{4.8}$$

At first we determine the function $\tilde{g}_1(r)$, which characterizes ESS, cf. Eq. (2.4). Figure 2 displays plots of $[S_q^u(r)/u_L^q]^{1/\zeta(q)}$ according to Eq. (2.3) for (a) the data A and (b) the data B, both vs r/L. The data should lie on one curve irrespective of q, provided that there exists a universal scaling function $\tilde{g}_1(r)$ in Eq. (2.3). The curves for different q indeed nearly coincide. The slight q dependence at large r seems to be compatible with the statistical scatter, since one cannot see a systematic q dependence. In a previous paper [12] we used the assumption that $r\tilde{g}_1(r)$ is monotonously increasing with r; this property clearly is fulfilled with the data of both sets.

We now consider the scaling function $\tilde{f}(r)$, relevant for the crossover from the viscous to the inertial subranges. Figure 3 shows the plots of the rhs of Eq. (4.6), representing $\tilde{f}(r)$. Here we used the expression in terms of $\zeta(q)$ and $\zeta(p)$ as experimentally observed. There is a systematic q dependence in the viscous subrange in the numerical simulation data, cf. Fig. 3(a). We kept fixed $p=3$, because we did not observe sensitivity to the various p values, which we checked. In the jet data (data B) the function $\tilde{f}(r)$ show statistical fluctuations for $r^* \geqslant 10$, but no apparent q dependence. But again we note systematic deviations in the small scale range $r^* \leqslant 10$. Thus a universal scaling functions $\tilde{f}(r)$ seems to only approximately exist. Incidentally, it is a monotonously increasing function of r, which also satisfies the expected asymptotics (2.18). The considerable scatter in the data for $r^* \leqslant 5$ in Fig. 3(b) may be due to statistical errors in the sampling of the data because of the short time scales related with these small spatial scales.

The numerical and experimental results for $r\tilde{g}_1(r)$ as given by Eq. (4.7) are shown in Fig. 4. Here we used the expression in terms of $\zeta(q)$ and $\zeta(p)$ as experimentally observed. One can distinguish three characteristic r ranges, which we naturally identify with the viscous, the inertial, and the stirring subranges: (i) First the VSR for $r^* \leqslant 10$, where we expect that $r\tilde{g}_1(r)$ approaches a constant as the scale r is decreased. (ii) An intermediate range, where $r\tilde{g}_1(r)$ is roughly proportional to r. (iii) The large r range, where $r\tilde{g}_1(r)$ again approaches a constant as the scale is increased. Although the jet results (data B) contain considerable statistical fluctuations, it seems that they do not systematically depend on q except again toward the viscous subrange. Because the q dependences in the small scale regions in both Figs. 4(a) and 4(b) can be spoiled by insufficient data sampling in the numerical simulation and in the jet experiment due to the short time scales, one cannot safely draw, from the present data, the conclusion that there does not exist a universality in the VSR. The deviations at the large scales may be influenced by finite size effects, e.g., by the shape dependence of the flow container.

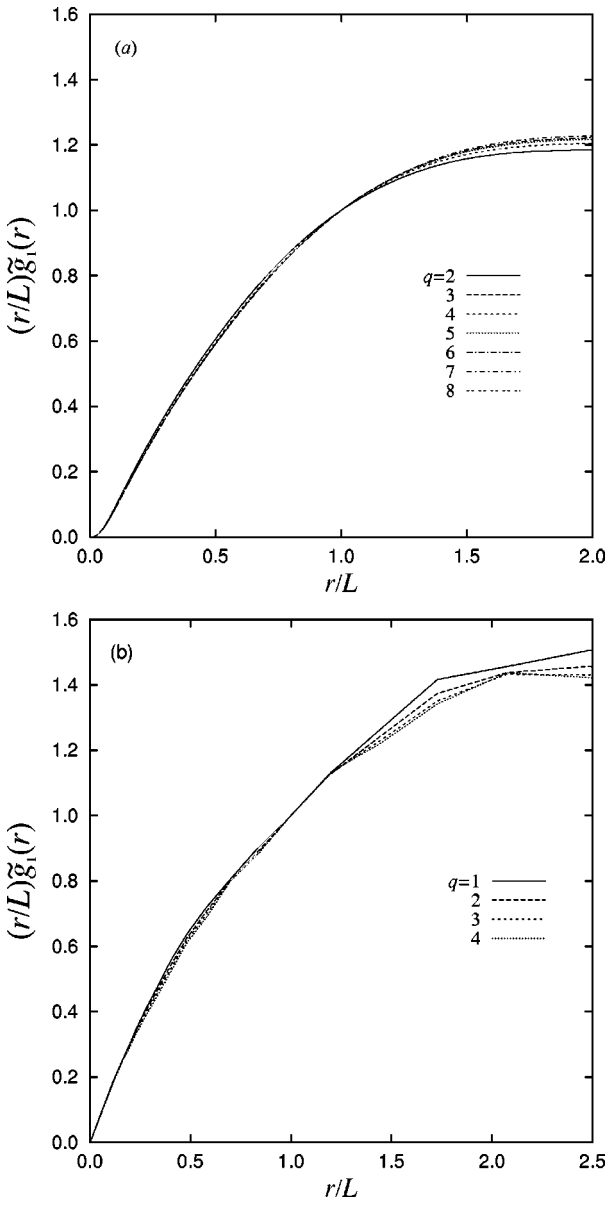

FIG. 2. Check of universality of $\tilde{g}_1(r)$ in the ESS formula (2.3) with (a) data A and (b) data B. Plotted is $[S_q^u(r)/u_L^q]^{1/\zeta(q)}$ vs r/L from Eq. (2.3) for several values of the moment order q. No apparent q dependence is observed in the graphs.

Next we determine the probability density $P_r(\epsilon)$ from the data . Then the fluctuation spectrum $S_{\hat{r}}(z)$ can be calculated too from Eq. (3.16) as

$$S_{\hat{r}}(z) = \frac{\ln[\sqrt{\ln(L/\hat{r})}\,\epsilon P_r(\epsilon)]}{\ln(\hat{r}/L)} + \text{const.} \tag{4.9}$$

Here $\hat{r} = r\tilde{g}_1(r)$ and $z = \ln(\epsilon/\epsilon_L)/\ln(L/\hat{r})$, see Eq. (3.17). Figure 5(a) shows the fluctuation spectrum $S_{\hat{r}}(z)$ for the data B

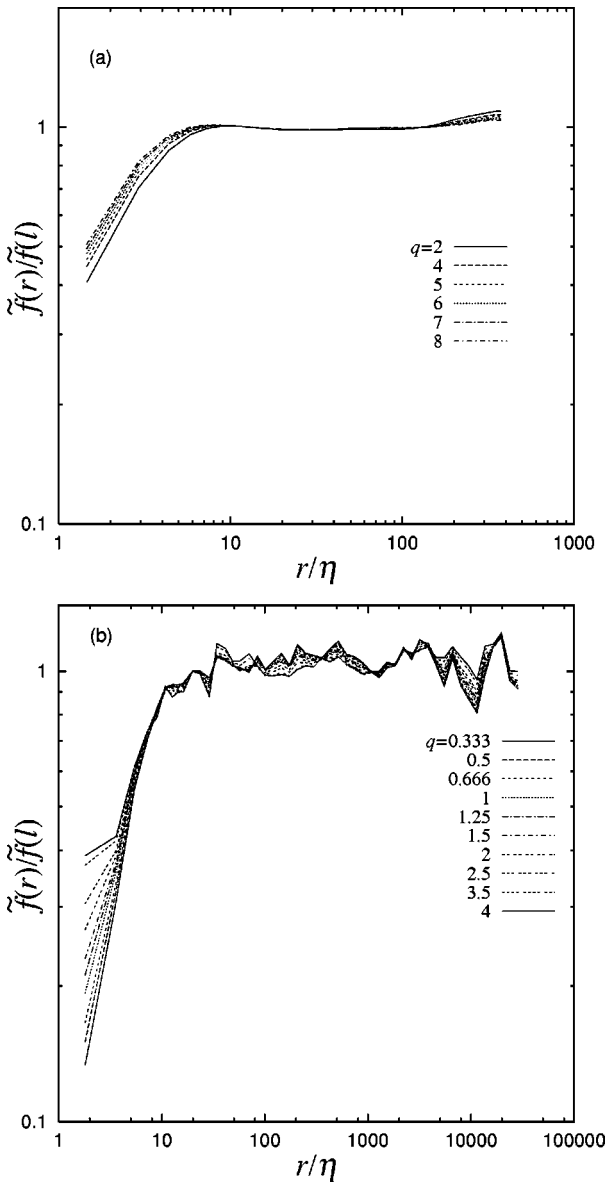

FIG. 3. Plots of the rhs of Eq. (4.6) for $p=3$ and various q as functions of $r^*=r/\eta$, normalized by its value at $r^*=a=l/\eta$. (a) The DNS, data A, (b) the jet measurements, data B.

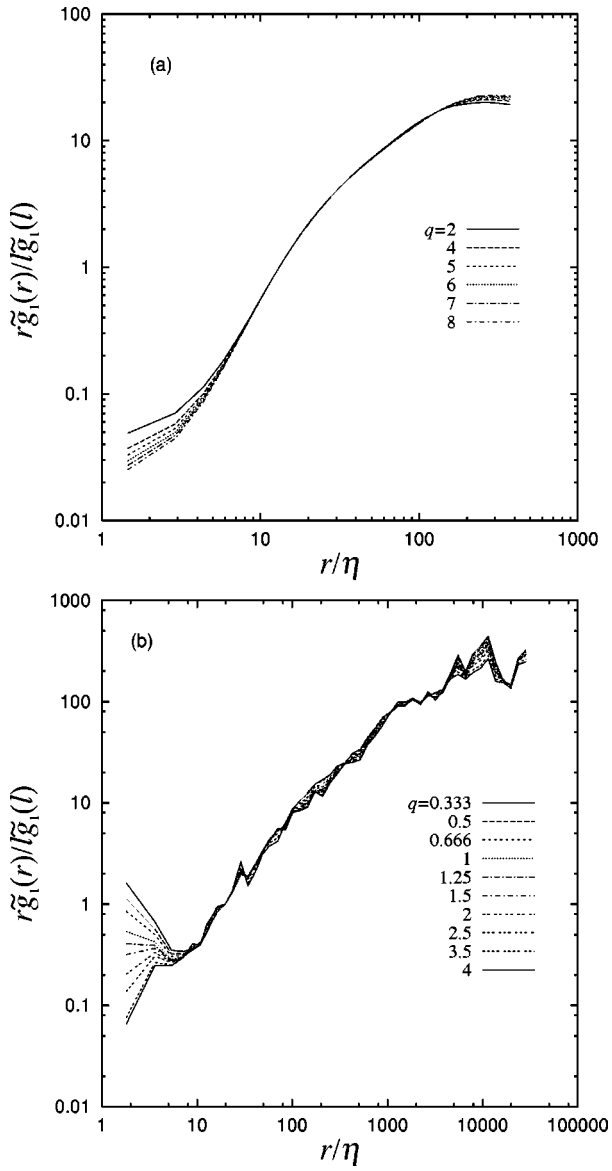

FIG. 4. Plots of the GESS representation (4.7) of the function $\tilde{g}_1(r)$ vs $r^*=r/\eta$, for different moment orders q and fixed $p=3$. As before (a) data A and (b) data B, and also normalized by their values at the viscous inertial crossover $a=l/\eta$.

(jet) calculated with Eq. (4.9), where the function $\hat{r}=r\tilde{g}_1(r)$, obtained from $G_{2,3}(r)$ as $r\tilde{g}_1(r)/L=[G_{2,3}(r)]^{1/[\zeta(2)-2\zeta(3)/3]}$, was used, [cf. Eq. (2.12)] and inserting (2.15). The r values were all chosen to be in the ISR; therefore, these $S_{\hat{r}}(z)$ characterize the fluctuations in the inertial subrange. Figure 5(b) offers the fluctuation spectra $S_r(z)$ calculated with r instead of $\hat{r}$ in Eqs. (4.9) and (3.16) in the same r range as in Fig. 5(a), i.e., calculated by assuming

$$P_r(\epsilon)\sim\frac{\epsilon^{-1}}{\sqrt{\ln\frac{L}{r}}}\left(\frac{r}{L}\right)^{S_r(z_r(\epsilon))}, \tag{4.10}$$

$$z_r(\epsilon)\equiv\frac{\ln\frac{\epsilon}{\epsilon_L}}{\ln\frac{L}{r}}. \tag{4.11}$$

If the inertial subrange is sufficiently extended, we expect that Figs. 5(a) and 5(b) coincide. However, one observes a weak disagreement of both, particularly on the left sides of the curves. Furthermore, the scatter in the data on the left sides of the curves in Fig. 5(b) is more significant than that in Fig. 5(a). We conclude from this observation that the asymptotic forms (3.16) and (3.17) with $\hat{r}$ are more favorable than that fitted as in Eqs. (4.10) and (4.11) with r. This means that $S_{\hat{r}}(z)$ is more fundamental than $S_r(z)$ to discuss

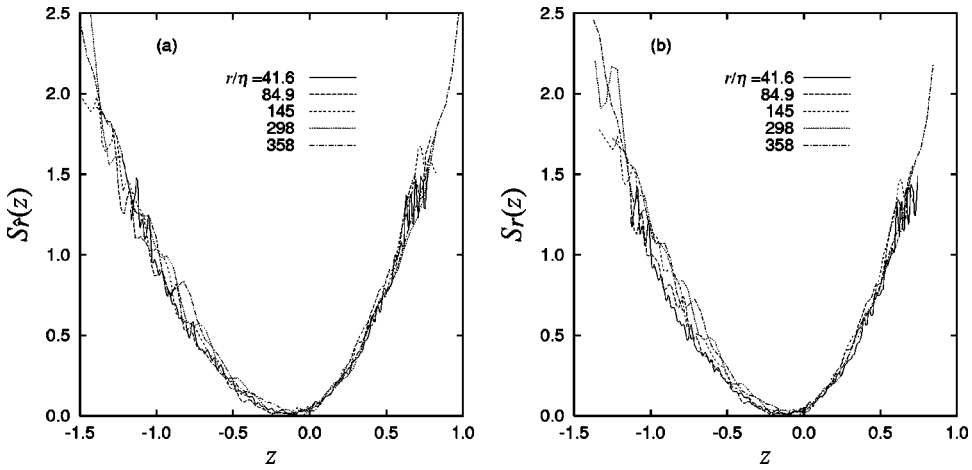

FIG. 5. Fluctuation spectra $S_{\hat{r}}(z)$ calculated in the inertial subrange with the same data (data *B*) but in two different ways. (a) With Eq. (4.9), equivalent to Eq. (3.16); $\hat{r}$ was calculated with $G_{2,3}(r)$. (b) With Eqs. (4.10) and (4.11) based on r.

the ISR scaling. In the next paragraph we shall check this in a more precise analysis by studying the differences of fluctuation spectra for two scales.

In order to study to which extent the fluctuation spectra $S_{\hat{r}}(z)$ and $S_r(z)$ depend on the scale r, we consider various differences $\Delta_{\hat{r}_1,\hat{r}_2}S(z) \equiv S_{\hat{r}_1}(z) - S_{\hat{r}_2}(z)$ and $\Delta_{r_1,r_2}S(z) \equiv S_{r_1}(z) - S_{r_2}(z)$ as functions of z for some pairs of different scales $r_i^* = r_i/\eta$, see Fig. 6. In Fig. 6(a) the scales are described by $\hat{r}$, while in Fig. 6(b) r is used. The pretty irregular scatter of the differences around zero seems to indicate that on average there is no significant r dependence of the fluctuation spectra $S_r(z)$. It therefore makes sense to speak of *the* spectrum $S(z)$ in the inertial subrange. Of course, the differences $\Delta S(z)$ are smaller in the vicinity of the minima of $S_{\hat{r}}(z)$ and $S_r(z)$ than for larger $|z|$, because the corresponding S values themselves are smaller or larger there.

A closer inspection of Fig. 6 shows that in Fig. 6(b) the differences on the left wing seem to have a systematic nonzero trend, in contrast to the right wing, but in particular in contrast to the symmetric scatter around zero in Fig. 6(a). We conclude that $S_{\hat{r}}(z)$ is less scale dependent than $S_r(z)$, i.e., Eq. (3.16) is more appropriate than Eq. (4.10).

Figures 7(a) and 7(b) show the fluctuation spectra in the crossover range between the inertial and the viscous subranges calculated with Eqs. (3.16) and (4.10), respectively. One again observes a considerable statistical scatter in the left side branches of the fluctuation spectra, while the right side branches seem to be robust against changing r to smaller scales. The more significant scatter on the left side wing in Fig. 7(b) as compared with that in Fig. 7(a) again supports the greater feasibility of the effective scale $\hat{r}$ in comparison to r itself. Furthermore it seems that the left side branch of $S_{\hat{r}}(z)$ in Fig. 7(a) becomes smaller as the scale r becomes smaller, which implies that the probability densities Q or P for the case of negative z and r in the viscous range [cf. Fig. 7(a)] are larger than in the inertial subrange [cf. Fig. 5(a)]. This fact coincides with an observation reported in Ref. [28] in the study of the GOY shell model.

To analyze the scale dependence in the crossover range we once more consider the spectra differences $\Delta_{\hat{r}_1,\hat{r}_2}S(z)$ and $\Delta_{r_1,r_2}S(z)$. Here r_2 is kept fixed at $r_2 = 173\eta$ in the ISR, while r_1 is stepwise reduced from 101η down to 9.03η. As before, Figs. 8(a) and 8(b) differ in being based on Eq. (3.16) with $\hat{r}$ and on Eq. (4.10) with r, respectively. In Figs. 8(c) and 8(d) the corresponding curves have been smoothened with Bezier curves in the data-plotting tool, the gnuplot. It becomes apparent that the smaller the scale is, the more $S_r(z)$ deviates from $S_{173\eta}(z)$. We have to conclude that the fluctuation spectra in the VSR with decreasing r gradually deviate from those in the ISR. Particularly their left branch tends to decrease as the scale becomes smaller. This observation is less pronounced if $P_{\hat{r}}(\epsilon)$ is taken, Fig. 8(c), than with $P_r(\epsilon)$, see Fig. 8(d).

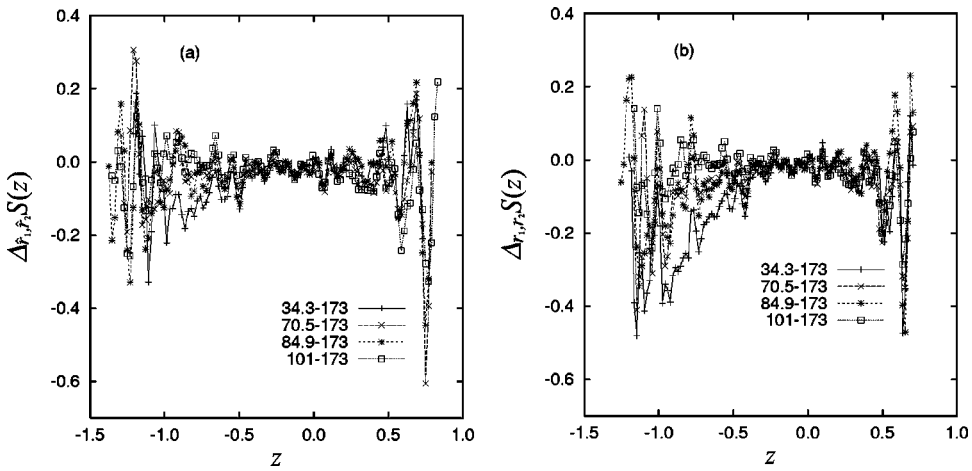

FIG. 6. Differences $\Delta_{\hat{r}_1,\hat{r}_2}S(z) = S_{\hat{r}_1}(z) - S_{\hat{r}_2}(z)$ and $\Delta_{r_1,r_2}S(z) = S_{r_1}(z) - S_{r_2}(z)$ of the fluctuation spectra vs z for four scale differences within the inertial subrange. (a) and (b) were calculated with Eq. (3.16), referring to $\hat{r}$, and Eq. (4.10), referring to r itself, respectively. The scales $r_1/\eta = 34.3, 70.5, 84.9$, and 101 are compared with $r_2/\eta = 173$.

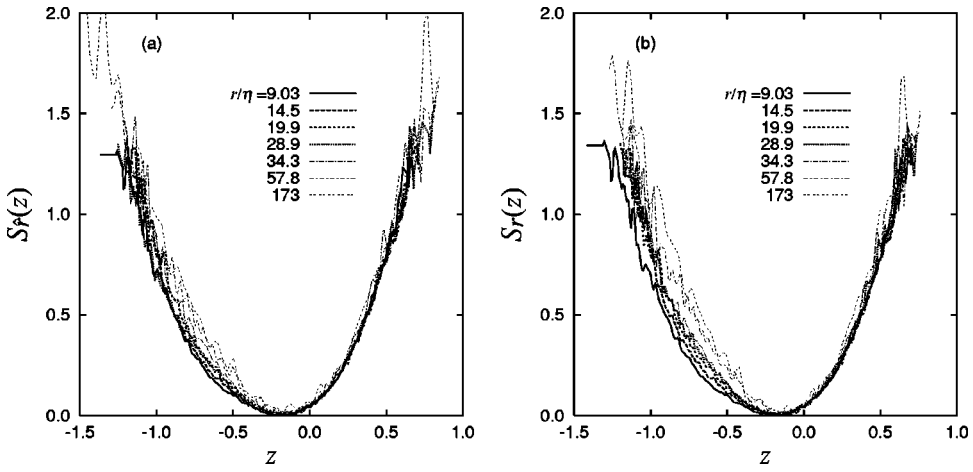

FIG. 7. Fluctuation spectra in the crossover region between the viscous and the inertial subranges. (a) is calculated with Eq. (3.16), i.e., parametrized with $\hat{r}$, and (b) with Eq. (4.10), based on r directly. The scatter of the data in (a) seems weaker than in (b). In (a), $\hat{r}(r)$ was calculated with $G_{2,3}(r)$.

Figure 9 displays the comparison of the measured fluctuation spectra with three analytical approximation formulas. Scales r in the lower ISR are considered. The jet data B are taken. The first analytical approximation is the parabolic fit (P) [2,23],

$$S(z)=\frac{D}{2}(z-z_0)^2. \tag{4.12}$$

z_0 is the minimum position, $S'(z_0)=0$, and D is the curvature at minimum, $D=S''(z_0)$. Both parameters z_0 and D are independent. This approximation corresponds to the quadratic excess exponent

$$\tau(q)=-z_0 q-\frac{q^2}{2D}. \tag{4.13}$$

The second analytic expression $(K62)$ is obtained from Kolmogorov and Obukhov's log normal theory [4,5], which again turns out to be quadratic in z and q. But since here $\tau(1)=0$ is taken into account (concluded from the structure

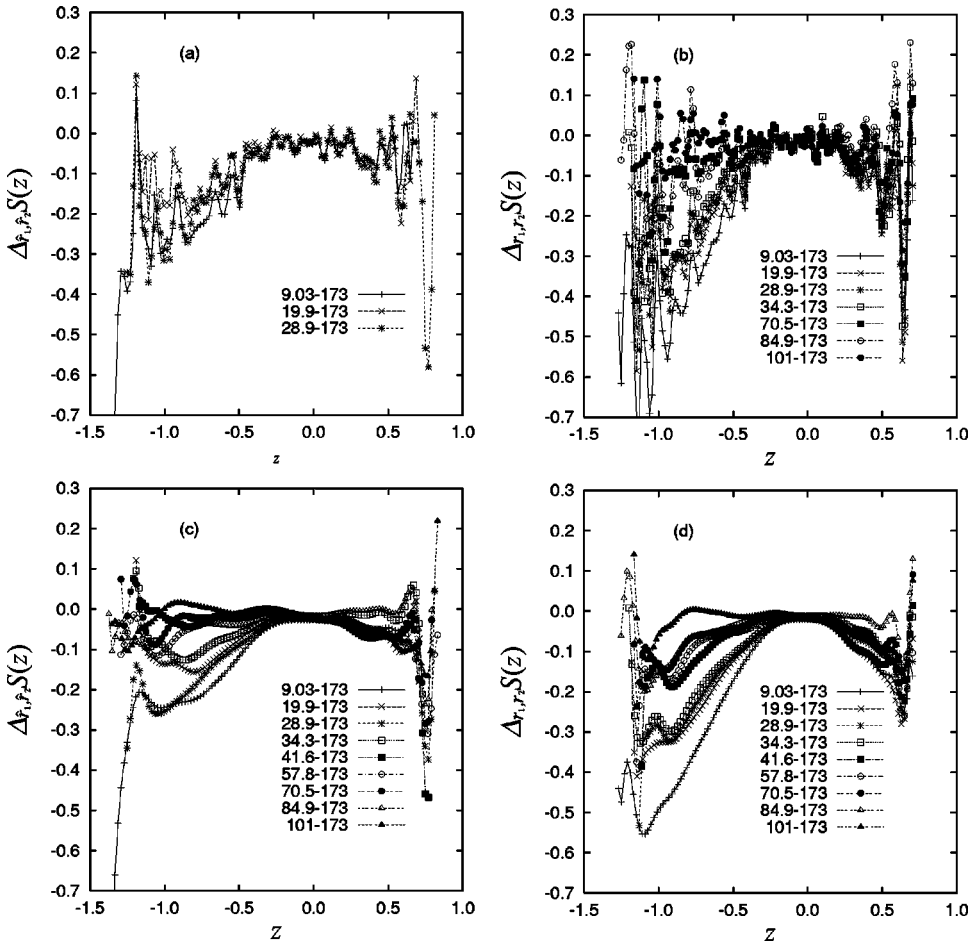

FIG. 8. (a) and (b) show differences $\Delta_{\hat{r}_1,\hat{r}_2}S(z)$ and $\Delta_{r_1,r_2}S(z)$ of the fluctuation spectra for various scales in the viscous and in the inertial subranges from $S_{\hat{r}_2}(z)$ with $r_2=173\,\eta$. (a) and (b) were calculated with Eqs. (3.16), (3.17) and with Eqs. (4.10), (4.11), respectively. (c) and (d) show the curves corresponding to those in (a) and (b), but smoothened with the Bezier method.

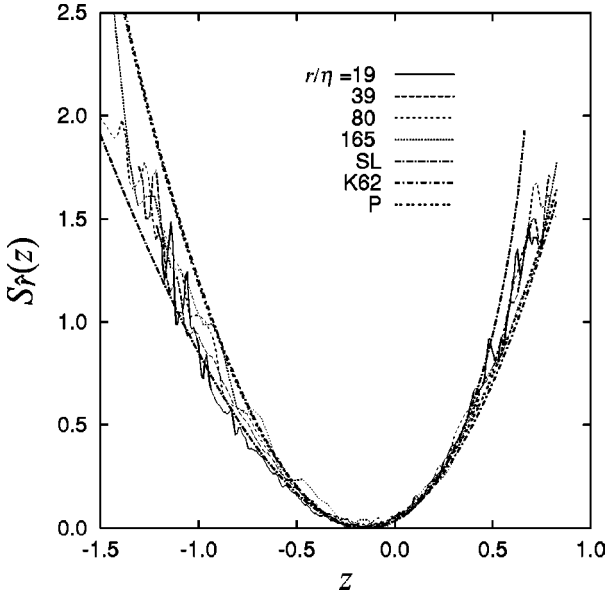

FIG. 9. Comparison of the fluctuation spectra obtained from the data B with the analytical approximation formulas. P is the parabolic fit with $D=3.35$ and $z_0=-0.161$ [Eq. (4.12)], $K62$ indicates Kolmogorov and Obukhov's log normal theory with $\mu=0.30$ [Eq. (4.15)], and SL denotes the She-Leveque model [Eq. (4.16)].

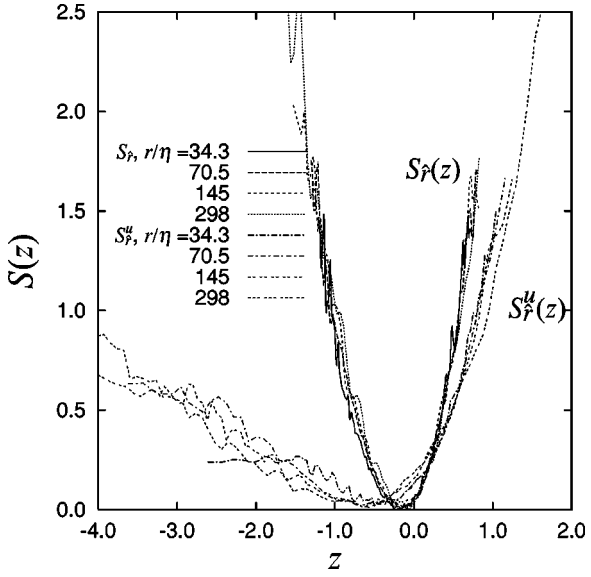

FIG. 10. Comparison of the fluctuation spectra obtained from $P_r(\epsilon)$ and $P_r(u)$. One observes that they are globally different from each other. In particular, the difference is remarkable in a negative z region. For details, see the text.

equation), z_0 and D are related, and only one parameter is left. As this we take $\mu\equiv-\tau(2)$, the intermittency exponent, and obtain

$$\tau(q)=\frac{\mu}{2}q(1-q), \tag{4.14}$$

thus

$$S(z)=\frac{1}{2\mu}\left(z+\frac{\mu}{2}\right)^2. \tag{4.15}$$

The third analytical expression comes from She-Leveque's log-Poisson model [29,23,31,30],

$$S(z)=2+\frac{1}{\ln\frac{3}{2}}\left(\frac{2}{3}-z\right)\ln\left[\frac{1}{2e\ln\frac{3}{2}}\left(\frac{2}{3}-z\right)\right]. \tag{4.16}$$

The intermittency excess exponent $\tau(q)$ is given by [29]

$$\tau(q)=-\frac{2}{3}q+2\left[1-\left(\frac{2}{3}\right)^q\right]. \tag{4.17}$$

Equation (4.16) implies the minimum position and the curvature,

$$z_0=\frac{2}{3}-2\ln\frac{3}{2}\approx-0.144, \tag{4.18a}$$

$$S''(z_0)=\left(2\ln^2\frac{3}{2}\right)^{-1}\approx 3.04. \tag{4.18b}$$

As mentioned, the comparison of the measured spectra with the three analytical models is presented in Fig. 9.

Let us discuss the probability densities $P_r(\epsilon)$ and $P_r(u)$. The comparison of $\tau(q)$ from energy-dissipation rate fluctuations with that obtained by assuming (1.10) from velocity structure functions for data B is given in Fig. 1(b). One observes a remarkable difference. This may suggest the inapplicability of the GERSH in a rigorous sense. However, if the characteristic function $\zeta(q)/\zeta(3)$ is used instead of $\zeta(q)$ itself, the result approximately coincides with the curve $\tau(q)$. This implies that the relation (1.10) holds for small q in the range shown in Fig. 1(b). Furthermore, the fluctuation spectra $S_{\hat{r}}(z)$ calculated with $P_r(\epsilon)$ and $P_r(u)$ are compared in Fig. 10. If the GERSH holds, they collapse on a same curve at least approximately. Clearly, one observes a remarkable difference of the spectra on the left side of the curves. A small value of the exponent $z_{\hat{r}}$ corresponds to a small value of u_r or ϵ_r. The probability density $P_r(u)$ does not vanish for small value of u. On the other hand, the probability density $P_r(\epsilon)$ practically vanishes for small value of ϵ. This is the reason why the characteristic of $S^u_{\hat{r}}(z)$ and $S_{\hat{r}}(z)$ observed with $P_r(\epsilon)$ is different. However, in addition, the curves on the right side are different from each other. For a small value of q, as shown in Fig. 1(b), no clear difference of the characteristic function $\zeta(q)$ calculated with $P_r(u)$ and $P_r(\epsilon)$ for q in the range in Fig. 1(b) is observed. It is expected that the difference of the $\zeta(q)$ calculated in two ways, will be enhanced as q is increased, reflecting the difference of $S_{\hat{r}}(z)$ and $S^u_{\hat{r}}(z)$ and $S_{\hat{r}}(z)$. One thus concludes that the fluctuation spectrum $S_{\hat{r}}$ is more sensitive than the character-

istic function $\zeta(q)$ itself. The difference of $S_{\hat{r}}(z)$ and $S_{\hat{r}}(z^{(u)})$ implies that the GERSH is not valid in a rigorous sense. Therefore, Eq. (3.13) only holds for small q. Nevertheless, the asymptotic forms (3.16) and (3.24) hold independently.

V. CONCLUDING REMARKS

In the present paper, we presented the derivation of the generalized extended self-similarity formulas, GESS, of turbulent flow structure functions. This GESS is supposed to bridge the statistical behavior in the viscous, the inertial, and the stirring subranges. The approach is based on the $K62$ similarity theory of developed turbulence [4]. The main differences between the present derivation of GESS and the $K62$ theory are first to carry out the self-similarity analysis not for the physical scale r itself but for the effective scale $\hat{r}$, defined in Eq. (3.5), and second to apply the large deviation theory instead of the central limit theorem. In addition, we proposed the asymptotic form of the probability densities $P_r(\epsilon)$ and $P_r(u)$, for which the fluctuation spectra $S_{\hat{r}}(z)$ play the most important role, compatible with GESS. The peculiarities of the obtained probability densities are that (i) they take the generalized form of the $K62$ log normal theory, and (ii) there appears an effective scale $\hat{r}$ instead of the physical scale r. Furthermore, using Katsuyama *et al.*'s data [25,26], measured in an air-in-air jet flow, we constructed the fluctuation spectra $S_{\hat{r}}(z)$, see Eq. (3.16), also consistent with GESS. We evaluated the fluctuation spectrum $S^u_{\hat{r}}(z^{(u)})$ with the probability density $P_r(u)$ from Katsuyama's data, and found a remarkable difference between $S_{\hat{r}}(z)$ and $S^u_{\hat{r}}(z^{(u)})$. This fact implies the breakdown of the GERSH in a rigorous sense although the characteristic functions $\tau(q)$ for small values of q calculated with the ESS processing seem to coincide with each other. One should study the applicability of the RSH, the ERSH, and the GERSH more carefully.

Our analyses of two data sets do not sufficiently confirm the validity of our approach toward the viscous scales. However, they also do not indicate its inapplicability toward the viscous range since the experimental data have limited precision for the small scales: In data *A*, the ratio $\eta/\Delta x$ with the grid size Δx used in DNS is $2.03/2\pi \approx 1/3$. In data *B*, the smallest eddies time scale $\tau(=10\sqrt{\nu/\epsilon_L})$ is 4 ms, which should be compared with the sampling time $\Delta t = 10$ μs. Although τ is 400 times larger than Δt, the spatial resolution $(=U\Delta t = 140$ μm) is twice the Kolmogorov scale $\eta($ $=80$ μm). One needs, therefore, more and more accurate experiments to finally confirm the validity of the present approach as well as the applicability of GESS also toward the VSR.

As pointed out in Ref. [10], GESS is specified by two functions $\tilde{f}(r)$ and $\tilde{g}_1(r)$ as in Eq. (2.15). The function $\tilde{f}(r)$ plays an important role in the crossover region between the dissipative and the inertial subranges. Therefore, it is natural to assume that the function $\tilde{f}(r)$ is a unique function of r/l, i.e.,

$$\tilde{f}(r) = f\left(\frac{r}{l}\right). \tag{5.1}$$

On the other hand, the function $\tilde{g}_1(r)$ depends on both l and L. Since there appears no characteristic scale except these two scales, $\tilde{g}_1(r)$ may be written as

$$\tilde{g}_1(r) = g_1\left(\frac{r}{l}, \frac{r}{L}\right) \tag{5.2}$$

with a unique function $g_1(x,y)$ of x and y. The scaling functions f and g_1 have the asymptotic forms $f(x) = c_1 x$ for $x \ll 1$ and c_2 for $x \gg 1$, and $g_1(x,y) = c_3 x^{-1}$ for $x \ll y \ll 1$ and $g(y)$ for $y \gg x \gg 1$, where c_1, c_2, and c_3 are numerical constants of $O(1)$, cf. Eq. (2.18). Using the direct numerical simulation data by Fukayama *et al.* [24] and the experimental data by Katsuyama *et al.* [25,26], we determined the functions $\tilde{f}$ and $\tilde{g}_1$. Numerical analysis suggests the q independent, universal existence of such functions. Although we analyzed two data sets, it still is considered as insufficient to draw a firm conclusion on the universality of the functions $f(x)$ and $g_1(x,y)$. It still remains an attractive problem to clarify and confirm their universality. Further numerical and experimental studies are highly desired. Possible forms of $f(x)$ and $g_1(x,y)$ in connection with the Batchelor and the Lohse and Müller-Groeling parametrizations for $S^u_2(r)$ are proposed in Appendix B.

The function $S(z)$ is simply related to the multifractal spectrum $h(z)$ [20], where $h(z)$ is defined as the fractal dimension of the support where $\overline{z_r}$ takes the value z [2,31,12], as

$$h(z) = 3 - S(z). \tag{5.3}$$

It is worthy to note that $h(z)$ can be negative. In contrast to measuring $S(z)$, it is not possible to directly observe the multifractal spectrum $h(z)$, which has been determined by using the Legendre transform of the exponent function $\zeta(q)$. The present $S(z)$ can be directly measured as shown in Sec. IV. In this sense, the present approach is more convenient than the multifractal picture in analyzing turbulent flow.

ACKNOWLEDGMENTS

The authors wish to thank the Japan Society for the Promotion of Science (JSPS). The present work was initiated when S.G. stayed in Kyoto as an invited foreign researcher supported by the short-term program of JSPS. The authors thank Professor Tomoo Katsuyama and Dr. Daigen Fukayama for providing their experimental and numerical data. This study was partially supported by Grant-in-Aid for Scientific Research No. 11837009 from the Ministry of Education, Science, Sports and Culture of Japan. T.W. was supported by the JSPS.

APPENDIX A: SELF-CONSISTENT EQUATION FOR THE PROBABILITY DENSITY OF ϵ_r

Let L and η be the energy injection scale and the Kolmogorov viscous length $\eta=(\nu^3/\epsilon_L)^{1/4}$. Three scales r_1, r_2, and r_3 are chosen such that $\eta<r_3<r_2<r_1\leqslant L$. We introduce an effective scale $\hat{r}\equiv\hat{r}(r)$ for later convenience. $\hat{r}(r)$ is assumed to be a monotonous function of r, i.e., $\hat{r}'(r)>0$, but at present not specified further.

Let $P(\epsilon_j,r_j|\epsilon_k,r_k)$, $r_j<r_k$, be the conditional probability density that the coarse-grained energy-dissipation rate averaged over the scale r_j takes the value ϵ_j under the condition that the coarse-grained energy-dissipation rate averaged over the scale r_k takes the value ϵ_k. In order to mathematically formulate the self-similar characteristics of large Reynolds number turbulence, we assume that the following self-consistent ansatz for the conditional probability densities holds:

$$P(\epsilon_3,r_3|\epsilon_1,r_1)=\int P(\epsilon_3,r_3|\epsilon_2,r_2)P(\epsilon_2,r_2|\epsilon_1,r_1)d\epsilon_2. \tag{A1}$$

This equation expresses first, that the probability density for the scales r_1 and r_2 propagates into that for r_1 and r_3. Second, the self-similarity hypothesis for the energy-dissipation rate fluctuations states that the propagator should be equal to the conditional probability density for the scales r_2 and r_3. Ansatz (A1) looks like the Chapman-Kolmogorov type equation for the velocity probability density proposed in Ref. [32].

Next, we turn to solving the self-consistent equation (A1) for large Re, i.e., for a sufficiently extended inertial subrange. Consider the case that the effective distances satisfy the relations $\hat{r}_3\ll\hat{r}_2\ll\hat{r}_1$. In this case, Eq. (A1) has two types of asymptotic, large Re solutions.

The first type solution takes the form

$$P(\epsilon_j,r_j|\epsilon_k,r_k)\sim\left[\ln\left(\frac{\hat{r}_k}{\hat{r}_j}\right)\right]^{-1/2}\epsilon_j^{-1}\left(\frac{\hat{r}_k}{\hat{r}_j}\right)^{-S(z(\epsilon_j,r_j|\epsilon_k,r_k))} \tag{A2}$$

for $\hat{r}_j\ll\hat{r}_k$ with

$$z(\epsilon,\hat{r}|\epsilon',\hat{r}')=\frac{\ln\dfrac{\epsilon}{\epsilon'}}{\ln\dfrac{\hat{r}'}{\hat{r}}}, \tag{A3}$$

where $S(z)$ is a non-negative and concave function,

$$S(z)\geqslant 0,\quad S''(z)>0. \tag{A4}$$

The prefactor in Eq. (A2) comes from the normalization condition $\int P(\epsilon_j,r_j|\epsilon_k,r_k)d\epsilon_j=1$ and is irrelevant for the asymptotic form of the probability density. This can be shown below. Let us put

$$\hat{r}_j=\hat{r}_L e^{-n_j},\quad x_j=\ln\frac{\epsilon_j}{\epsilon_L}, \tag{A5}$$

where $\hat{r}_L$ and ϵ_L are reference values of the effective scale and the coarse-grained energy-dissipation rate, respectively. Inserting Eq. (A2) with Eq. (A5) into Eq. (A1) yields

$$\begin{aligned}\exp\left[-S\left(\frac{x_3-x_1}{n_3-n_1}\right)(n_3-n_1)\right]&\sim\int_{-\infty}^{\infty}\exp\left[-S\left(\frac{x_3-x_2}{n_3-n_2}\right)(n_3-n_2)\right.\\&\left.-S\left(\frac{x_2-x_1}{n_2-n_1}\right)(n_2-n_1)\right]dx_2.\end{aligned} \tag{A6}$$

Here, we neglected the prefactor in Eq. (A2), because it contributes only logarithmically to the asymptotic form of the probability density. In saddle point approximation, corresponding to the condition

$$S'\left(\frac{x_3-x_2^*}{n_3-n_2}\right)=S'\left(\frac{x_2^*-x_1}{n_2-n_1}\right), \tag{A7}$$

Eq. (A6) implies

$$\begin{aligned}S\left(\frac{x_3-x_1}{n_3-n_1}\right)(n_3-n_1)=&S\left(\frac{x_3-x_2^*}{n_3-n_2}\right)(n_3-n_2)+S\left(\frac{x_2^*-x_1}{n_2-n_1}\right)\\&\times(n_2-n_1),\end{aligned} \tag{A8}$$

for the function S. Here x_2^* is the value of x_2 that maximizes the integrand of Eq. (A6), and is determined by $(x_3-x_2^*)/(n_3-n_2)=(x_2^*-x_1)(n_2-n_1)$, because $S(z)$ is a concave function.

Let us now evaluate the moments of the energy-dissipation rate fluctuations, $\langle\epsilon_r^q\rangle$. Assuming that the energy-dissipation rate at scale L does not fluctuate, the order q moments of ϵ_r for $r<L$,

$$\langle\epsilon_r^q\rangle=\int\epsilon^q P(\epsilon,r|\epsilon_L,L)d\epsilon, \tag{A9}$$

are governed by the fluctuation statistics of the scales r less than L. From Eq. (A1), we find

$$\langle\epsilon_{r_3}^q\rangle=\int\left[\int\epsilon_3^q P(\epsilon_3,r_3|\epsilon_2,r_2)d\epsilon_3\right]P(\epsilon_2,r_2|\epsilon_L,L)d\epsilon_2. \tag{A10}$$

Substituting the asymptotic probability density (A2) into Eq. (A10), the factor $[\cdots]$ is evaluated with steepest descent as

$$\begin{aligned}[\cdots]&\sim\int\epsilon_3^q\epsilon_3^{-1}\left(\frac{\hat{r}_2}{\hat{r}_3}\right)^{-S(\ln(\epsilon_3/\epsilon_2)/\ln(\hat{r}_2/\hat{r}_3))}d\epsilon_3\\&\sim\epsilon_2^q\int\left(\frac{\hat{r}_2}{\hat{r}_3}\right)^{qz-S(z)}dz\sim\epsilon_2^q\left(\frac{\hat{r}_2}{\hat{r}_3}\right)^{-\tau(q)},\end{aligned} \tag{A11}$$

where we defined

$$\tau(q)=\min_{z}[S(z)-qz]. \tag{A12}$$

The moments (A9) are thus written as

$$\langle \epsilon_{r_3}^q \rangle \sim \left(\frac{\hat{r}_2}{\hat{r}_3}\right)^{-\tau(q)} \langle \epsilon_{r_2}^q \rangle,$$

which implies the asymptotic form

$$\langle \epsilon_r^q \rangle \sim \epsilon_L^q \left(\frac{\hat{r}}{\hat{L}}\right)^{\tau(q)}. \tag{A13}$$

Here we used the boundary condition at $r=L$ and noticed again that the fluctuations of ϵ_r over the scale L are zero (or at least sufficiently small).

The second type solution to Eq. (A1) is the power law

$$P(\epsilon_j,r_j|\epsilon_k,r_k)\sim\left(\frac{\epsilon_j}{\epsilon_k}\right)^{\lambda}, \quad \lambda \text{ a constant.} \tag{A14}$$

If Eq. (A14) is written in the form of Eq. (A2), we find that $S(z)$ depends linearly on z,

$$S(z)=(\lambda+1)z+\text{const.} \tag{A15}$$

However, we do not observe this type of behavior in our numerical and experimental analyses in Sec. IV.

APPENDIX B: POSSIBLE FORMS OF SCALING FUNCTIONS $\tilde{f}$ AND $\tilde{g}_1$

In fully developed turbulence, if the scale r is chosen within a sufficiently broad range between η and L, no effects from the stirring and the viscous subranges are significant, and we can put

$$\hat{r}(r)\equiv r\tilde{g}_1(r)=r. \tag{B1}$$

In the case of ESS, as proposed in Ref. [12], the function $\hat{r}(r)$ takes the form,

$$\hat{r}(r)=rg\left(\frac{r}{L}\right). \tag{B2}$$

Figure 2 numerically and experimentally proves $\hat{r}'(r)>0$. In the case of GESS, the effective scale $\hat{r}$ may be written in the scaling form,

$$\hat{r}(r)=rg_1\left(\frac{r}{l},\frac{r}{L}\right), \tag{B3}$$

where $g_1(x,y)$ is supposed to be a unique function of x and y. Figure 4 demonstrates the monotony property of $\hat{r}(r)$, namely, $\hat{r}'(r)>0$, except for $r^*\leqslant 10$. The data in Fig. 4(b) show a systematic deviation from $\hat{r}'(r)>0$. One possible explanation may be statistical errors in the sampling of the data, because the time scales on these small spatial scales are quite short. One has to reexamine the statistics on these scales with additional, other data.

Batchelor [27] proposed a parametrization for $S_2^u(r)$ bridging behaviors for $r\ll l$ and $r\gg l$. The Batchelor parametrization [27,18] is given in Eq. (4.2) and rewritten here as

$$S_2^u(r)\sim\left\{\frac{r}{l}\left[1+\left(\frac{r}{l}\right)^2\right]^{-1/2}\right\}^2\left[\frac{r}{L}\frac{\left[1+\left(\frac{r}{l}\right)^2\right]^{1/2}}{\frac{r}{l}}\right]^{\zeta(2)}, \tag{B4}$$

expected to hold for all $r\ll L$ including the crossover region between the viscous and the inertial subranges. Comparing this with the scaling relation (2.15) for $q=2$ with the assumption (B3), one obtains

$$f(x)=\frac{x}{\sqrt{1+x^2}}, \tag{B5a}$$

$$g_1(x,0)=\frac{\sqrt{1+x^2}}{x}. \tag{B5b}$$

In Ref. [12], we proposed the extended form of the Lohse and Müller-Groeling parametrization [33] that now bridges all three ranges, the viscous, the inertial, and the stirring subranges. The proposed form is

$$\begin{aligned} S_2^u(r)&=\frac{a^2}{15}(\epsilon_L\eta)^{2/3}\\ &\quad\times\frac{\left(\frac{r}{l}\right)^2}{\left[1+\left(\frac{r}{l}\right)^{\kappa_l}\right]^{[2-\zeta(2)]/\kappa_l}\left[1+\left(\frac{r}{L}\right)^{\kappa_L}\right]^{\zeta(2)/\kappa_L}},\\ &\sim\left[\frac{\frac{r}{l}}{\left[1+\left(\frac{r}{l}\right)^{\kappa_l}\right]^{1/\kappa_l}}\right]^2\left[\frac{r}{L}\frac{\left[1+\left(\frac{r}{l}\right)^{\kappa_l}\right]^{1/\kappa_l}}{\frac{r}{l}\left[1+\left(\frac{r}{L}\right)^{\kappa_L}\right]^{1/\kappa_L}}\right]^{\zeta(2)} \end{aligned} \tag{B6}$$

with positive κ_l and κ_L. If we put $\kappa_l=\kappa_L=2$, the interpolation formula (B6) specializes to that of Lohse and Müller-Groeling. Equation (B6) suggests that the scaling functions in Eqs. (5.1) and (5.2) should be chosen as

$$f(x)=\frac{x}{(1+x^{\kappa_l})^{1/\kappa_l}}, \tag{B7a}$$

$$g_1(x,y)=\frac{(1+x^{\kappa_l})^{1/\kappa_l}}{x(1+y^{\kappa_L})^{1/\kappa_L}}, \tag{B7b}$$

and, therefore,

$$g(y)=g_1(\infty,y)=\frac{1}{(1+y^{\kappa_L})^{1/\kappa_L}}. \tag{B8}$$

Note that Eqs. (B7a) and (B7b) give Eqs. (B5a) and (B5b), respectively, for $\kappa_l=\kappa_L=2$.

[1] A. S. Monin and A. M. Yaglom, *Statistical Fluid Mechanics* (MIT Press, Cambridge, MA, 1975).
[2] U. Frisch, *Turbulence—The Legacy of A. N. Kolmogorov* (Cambridge University Press, Cambridge, 1995).
[3] A. N. Kolmogorov, Dokl. Akad. Nauk SSSR **30**, 9 (1941).
[4] A. N. Kolmogorov, J. Fluid Mech. **13**, 82 (1962).
[5] A. M. Obukhov, J. Fluid Mech. **13**, 77 (1962).
[6] R. Benzi, S. Ciliberto, R. Tripiccione, C. Baudet, F. Massaioli, and S. Succi, Phys. Rev. E **48**, R29 (1993).
[7] R. Benzi, S. Ciliberto, C. Baudet, and G. R. Chavarria, Physica D **80**, 385 (1995).
[8] M. Briscolini, P. Santangelo, S. Succi, and R. Benzi, Phys. Rev. E **50**, R1745 (1994).
[9] R. Benzi, L. Biferale, S. Ciliberto, M. V. Struglia, and R. Tripiccione, Phys. Rev. E **53**, R3025 (1996).
[10] R. Benzi, L. Biferale, S. Ciliberto, M. V. Struglia, and R. Tripiccione, Physica D **96**, 162 (1996).
[11] V. Carbone, P. Veltri, and R. Bruno, Phys. Rev. Lett. **75**, 3110 (1995); A. Arneodo *et al.*, Europhys. Lett. **34**, 411 (1996); Z. Vörös, P. Kovács, Á. Juhász, A. Körmendi, and A. W. Green, Phys. Research Lett. **25**, 2621 (1998); A. Turiel, G. Mato, N. Parga, and J. P. Nadal, Phys. Rev. Lett. **80**, 1098 (1998); A. Basu, A. Sain, S. K. Dhar, and R. Pandit, *ibid.* **81**, 2687 (1998); A. Sain, Manu, and R. Pandit, *ibid.* **81**, 4377 (1998); M. S. Johansen, P. Alstrom, J. Borg, and M. T. Levinsen, Eur. Phys. J. B **11**, 665 (1999); R. Benzi, M. Marrocu, A. Mazzino, and E. Trovatore, J. Atmos. Sci. **56**, 3495 (1999); G. S. Lewis and H. L. Swinney, Phys. Rev. E **59**, 5457 (1999).
[12] H. Fujisaka and S. Grossmann, Phys. Rev. E **63**, 026305 (2001).
[13] S. Grossmann, D. Lohse, and A. Reeh, Phys. Rev. E **56**, 5473 (1997).
[14] H. Politano, A. Pouquet, and V. Carbone, Europhys. Lett. **43**, 516 (1998).
[15] Readers should note that the exponent z_r in Ref. [12] is given by $z_r=(1/3)(\overline{z_r}-1)$.
[16] S. Grossmann, D. Lohse, and A. Reeh, Phys. Fluids **9**, 3817 (1997).
[17] S. Grossmann, D. Lohse, and A. Reeh, Phys. Rev. E **61**, 5195 (2000).
[18] H. Effinger and S. Grossmann, Z. Phys. B: Condens. Matter **66**, 289 (1987).
[19] C. Meneveau, Phys. Rev. E **54**, 3657 (1996).
[20] G. Parisi and U. Frisch, in *Turbulence and Predictability in Geophysical Fluid Dynamics*, Proceedings of the International School of Physics ''Enrico Fermi,'' Varenna, 1983, p. 84, edited by M. Ghil, R. Benzi, and G. Parisi (North-Holland, Amsterdam, 1985).
[21] W. Stroock, *An Introduction to the Theory of Large Deviations* (Springer-Verlag, Berlin, 1984); R. S. Ellis, *Large Deviations and Statistical Mechanics* (Springer-Verlag, Berlin, 1985).
[22] H. Fujisaka and M. Inoue, Prog. Theor. Phys. **77**, 1334 (1987); Phys. Rev. A **39**, 1376 (1989).
[23] T. Watanabe and H. Fujisaka, J. Phys. Soc. Jpn. **69**, 1672 (2000).
[24] D. Fukayama, T. Oyamada, T. Nakano, T. Gotoh, and K. Yamamoto, J. Phys. Soc. Jpn. **69**, 701 (2000).
[25] T. Katsuyama, Y. Horiuchi, and K. Nagata, Phys. Rev. E **49**, 4052 (1994).
[26] T. Katsuyama, M. Inoue, and K. Nagata, Phys. Rev. E **51**, 5571 (1995).
[27] G. K. Batchelor, Proc. Cambridge Philos. Soc. **47**, 359 (1951).
[28] Y. Nakayama, T. Watanabe, and H. Fujisaka, Phys. Rev. E **64**, 056304 (2001).
[29] Z.-S. She and E. Leveque, Phys. Rev. Lett. **72**, 336 (1994); Z.-S. She and E. C. Waymire, *ibid.* **74**, 262 (1995).
[30] A more general formula than Eq. (4.16) is $\tau(q)=-\gamma q+d_0-C\beta^q$, where γ, d_0, C, and $\beta(<1)$ are positive parameters. Requiring the equalities $\tau(0)=\tau(1)=0$, we get $C=d_0=\gamma/(1-\beta)$. This gives the fluctuation spectrum
$$S(z)=\frac{z-\gamma}{\ln\beta}\left[\ln\left(\frac{z-\gamma}{d_0\ln\beta}\right)-1\right]+d_0.$$
Near the unique minimum of $S(z)$ it has, of course, the parabolic form (4.12) with $z_0=\gamma+d_0\ln\beta$ and $D=(d_0\ln^2\beta)^{-1}$. Employing the SL argument [29], we obtain $\gamma=\frac{2}{3}$, $d_0=2$, and $\beta=\frac{2}{3}$. For the derivation of the above form, see Ref. [23].
[31] T. Watanabe, Y. Nakayama, and H. Fujisaka, Phys. Rev. E **61**, R1024 (2000).
[32] St. Lück, J. Peinke, and R. Friedrich, Phys. Rev. Lett. **83**, 5495 (1999).
[33] D. Lohse and A. Müller-Groeling, Phys. Rev. Lett. **74**, 1747 (1995); D. Lohse and A. Müller-Groeling, Phys. Rev. E **54**, 395 (1996).